Astragaloside IV alleviates silica-induced pulmonary fibrosis via inactivation of the TGF-β1/Smad2/3 signaling pathway

NANNAN LI[1,2], KE WU[3], FEIFEI FENG[1], LIN WANG[4], XIANG ZHOU[5] and WEI WANG[1]

[1]Department of Respiratory Medicine, The Second Hospital, Cheeloo College of Medicine, Shandong University, Jinan, Shandong 250033; Departments of [2]Respiratory Medicine, [3]Cardiology, [4]Special Examination and [5]Anesthesiology, Central Hospital of Tai'an of Shandong Province, Tai'an, Shandong 271000, P.R. China

Received July 10, 2020; Accepted December 8, 2020

DOI: 10.3892/ijmm.2021.4849

Abstract. The aim of the present study was to investigate the anti-fibrotic effects of astragaloside IV (ASV) in silicosis rats, and to further explore the potential underlying molecular mechanisms. A silica-induced rat model of pulmonary fibrosis was successfully constructed. Hematoxylin and eosin and Masson's trichrome staining were performed to observe the pathological changes in lung tissues. Immunohistochemical analysis was used to assess the expression levels of Collagen I, fibronectin and α-smooth muscle actin (α-SMA). A hemocytometer and Giemsa staining were used to evaluate the cytological characteristics of the bronchoalveolar lavage fluid. ELISA was used to detect the levels of the inflammatory cytokines tumor necrosis factor-α, interleukin (IL)-1β and IL-6. Reverse transcription-quantitative PCR and western blotting were performed to detect the mRNA and protein expression levels of genes associated with the transforming growth factor (TGF)-β1/Smad signaling pathway. ASV alleviated silica-induced pulmonary fibrosis, and reduced the expression of collagen I, fibronectin and α-SMA. In addition, the results of the present study suggested that the ASV-mediated anti-pulmonary fibrosis response may involve reduction of inflammation and oxidative stress. More importantly, ASV suppressed silica-induced lung fibroblast fibrosis via the TGF-β1/Smad signaling pathway, thereby inhibiting the progression of silicosis. In conclusion, the present study indicated that ASV may prevent silicosis-induced fibrosis by reducing the expression of Collagen I, fibronectin and α-SMA, and reducing the inflammatory response and oxidative stress, and these effects may be mediated by inhibiting the activation of the TGF-β1/Smad signaling pathway.

Correspondence to: Professor Wei Wang, Department of Respiratory Medicine, The Second Hospital, Cheeloo College of Medicine, Shandong University, 247 Beiyuan Street, Jinan, Shandong 250033, P.R. China
E-mail: ww666sci@163.com

Key words: astragaloside IV, silicosis, pulmonary fibrosis, transforming growth factor-β1

Introduction

Silicosis is a disease caused by long-term exposure to a large amounts of free silica dust, characterized by diffuse nodular fibrosis of the lungs, which eventually damages lung function, leading to respiratory failure and even death (1). China has the largest population of patients with silicosis, and the annual direct economic losses caused by silicosis in the country amounts to >8 billion RMB. In developed countries, silicosis is also a significant occupational health concern (2,3). However, the pathogenesis of silicosis is currently unclear, and there is a lack of clinically effective therapeutic drugs (4,5). Therefore, it is crucial to study the pathogenesis of silicosis and explore novel preventative methods.

Silicosis is a complex chronic inflammatory process involving multiple cells (alveolar macrophages, alveolar epithelial cells, fibroblasts and lymphocytes, amongst others), cytokines and multiple mediators (6). Amongst these multiple factors, transforming growth factor (TGF)-β1 serves a key role. An increasing number of studies have demonstrated that TGF-β1 is a powerful fibrogenic cytokine, which serves an important regulatory role in cell proliferation, differentiation, migration, immune regulation and transformation of the extracellular matrix (ECM) in fibrotic diseases, and participates in tissue repair and fibrosis (7-9). In addition, several studies have suggested that gaining additional insight into biological events downstream of TGF-β1 signaling may lead to the identification of novel molecular targets for the treatment of silicosis and various other fibrotic lung conditions.

Since there are currently few treatments and medicines aimed at reversing silicosis or delaying disease progression, the potential efficacy of traditional Chinese medicines are increasingly being assessed (10). Astragaloside IV (ASV) is one of the primary active substances of *Astragalus membranaceus*, which has attracted significant attention due to its prominent immune-regulatory, anti-inflammatory, anti-asthmatic and anti-fibrotic properties (11). According to Yu *et al* (12), ASV can resist bleomycin (BLM)-induced pulmonary fibrosis by inhibiting oxidative stress and inflammatory response levels. Wang *et al* (13) also reported that ASV can reduce the progression of renal fibrosis by inhibiting the mitogen-activated protein kinase pathway and TGF-β1/Smad signaling pathways. However, there is lack of data regarding the effects of ASV on

silica-induced lung silicosis fibroblast fibrosis. Therefore, the aim of the present study was to investigate the effects of ASV on silicosis and explore its potential mechanisms using *in vivo* experiments, in the hope of identifying a novel potential target for the treatment of silicosis.

Materials and methods

Animals and groups. A total of 60 male Sprague Dawley rats, weighing 180-200 g were used in the present study. All rats had *ad libitum* access to standard rat feed and tap water. The animals were randomly divided into four groups (n=15 per group): i) Control group, 1 ml saline and 0.25 ml air; ii) ASV group, intraperitoneal injection of 20 mg/kg ASV; ii) silicosis model group, 1 ml silica dust suspension (50 mg/ml) and 0.25 ml air; and iv) silicosis model group + ASV, 1 ml silica dust suspension (50 mg/ml) and 0.25 ml air, followed by ASV injected intraperitoneally. The flowchart of the animal experimental procedures is shown in Fig. 1. The present study was approved by the Ethics Committee of The Second Hospital of Shandong University and all procedures were performed in strict accordance with the recommendations outlined in the Guide for the Care and Use of Laboratory Animals of the National Institutes of Health.

Silica-induced rat model. All animals were anesthetized with 1% pentobarbital sodium (35 mg/kg, Dainippon Sumitomo Pharma) and fixed on a 60˚ inclined board with the help of rubber bands. The tongue of the mice was pulled and held using blunt forceps. Under the head mirror, endotracheal intubation was performed using an epidural anesthesia catheter with a connector attaching it to a 1-ml syringe that was inserted into the trachea to the point of the tracheal bifurcation. The crystalline particles were suspended in normal sterile saline and the suspension (50 mg/ml) was vigorously mixed using a Stuart® vortex shaker (Cole-Palmer) prior to instillation. For pathological tissue extraction, the rats were anesthetized with 1% pentobarbital sodium (35 mg/kg, Dainippon Sumitomo Pharma) and fixed on the plate. After the bronchoalveolar lavage fluid (BALF) was collected, the rats were euthanized by bloodletting. Then the pathological organs were collected immediately after animal euthanasia.

Hematoxylin and eosin (H&E) staining. Briefly, the lung tissues were fixed in 4% paraformaldehyde for 24 h at 37˚C. Subsequently, they were embedded in paraffin and cut into 5 μm sections using a microtome. Dewaxing and dehydration were performed using xylene and ethanol aqueous solution, followed by H&E staining. The sections were stained with hematoxylin for 5 min and eosin for 3 min at 37˚C.

Masson's trichrome staining. The dewaxed deparaffinized 5-μm lung tissue sections were fixed in Bouin's solution overnight at 37˚C, washed twice with distilled water, and stained with Mayer's hematoxylin and acid Ponceau for 5 and 10 min at 37˚C, respectively, then rinsed with distilled water 3 times. Subsequently, the sections were dissolved in a 1% phosphomolybdic acid aqueous solution. After 10-15 min, the sample was transferred to aniline blue and stained at 37˚C for 20 min. Finally, the sections were rapidly dehydrated in 95% alcohol, followed by hyaluronic acidification with dimethylbenzene (DAB).

Bronchoalveolar lavage fluid (BALF) and inflammatory cell counting. A tracheal tube was inserted into the trachea with a sufficient volume of Hank's Balanced Salt Solution (1 ml each time) to collect BALF. Following BALF collection, one part of the re-suspended BALF cells were used for differential counting of inflammatory cells, including neutrophils, lymphocytes and macrophages, using Giemsa staining (15 min at 37˚C). The remaining re-suspended BALF cells were later used for calculating the total cell count using a hemocytometer.

Measurement of TNF-a, interleukin (IL)-1β and IL-6 levels by ELISA. Concentrations of IL-6 (cat. no. ab178013; Abcam), IL-1β (cat. no. ab214025; Abcam) and TNF-a (cat. no. ab181421; Abcam) in the lung tissues were assessed using commercially available ELISA kits (USCN Business Co., Ltd.) according to the manufacturer's protocol (14).

Evaluation of oxidative stress in tissues. Lung samples were homogenized in ice-cold 250 mM sucrose solution to determine the levels of malondialdehyde (MDA), reactive oxygen species (ROS), superoxide dismutase (SOD) and glutathione peroxidase (GSH-px). For the detection of MDA, the tissue was homogenized in 1 ml PBS. MDA was determined using the thiobarbituric acid reactive substance method, and catalase as described previously (15). For the detection of ROS, intracellular reactive levels were evaluated using dihydroethidium staining, as described previously (16). For the detection of SOD, nitroblue tetrazolium, riboflavin and tetrametyletylenediamine were used in accordance with the Beauchamp and Fridovich method (17). For the detection of GSH-px, the tissue antioxidant capacity was measured as described previously by Moron *et al* (18).

Immunohistochemical analysis. Briefly, endogenous peroxidase activity within the sections was quenched by incubating the sections with 3% H_2O_2 for 10 min after dewaxing and hydration. Lung tissues were incubated in a humidified chamber with primary antibodies directed against Collagen I (1:100; cat. no. AF7001; Affbiotech), fibronectin (1:100; cat. no. WL00712a; Wanleibio) and α-SMA (1:100; cat. no. WL02510; Wanleibio) overnight at 4˚C. On the following day, the lung tissues were washed with PBS and incubated with a IgG antibody (1:100; cat. no. ab150077; Abcam) at 37˚C for 45 min. In the negative controls, the primary antibody was replaced with PBS. Subsequently, tissues were counterstained with DAB.

Reverse transcription-quantitative PCR (RT-qPCR) analysis. Total RNA was isolated from lung tissues using TRIzol® reagent (Invitrogen; Thermo Fisher Scientific Inc.) and then the extracted RNA was reverse transcribed to cDNA using Sensiscript RT kit (Thermo Fisher Scientific, Inc.). The reverse transcription temperature protocol was denaturation at 70˚C for 10 min followed by reverse transcription at 42˚C for 15 min. Subsequently, qPCR was performed using BeyoFast™ SYBR Green qPCR mix (Beyotime Institute of Biotechnology) according to the manufacturer's protocol (19) The thermocycling conditions were as follows: 95˚C for 5 min;

Table I. Sequences of the primers.

Gene	Forward, 5'-3'	Reverse, 5-3'
Collagen I	TCCTGCCGATGTCGCTATCC	TCGTGCAGCCATCCACAAGC
Fibronectin	TCGCTTTGACTTCACCACCA	TGAGACCCAGGAGACCACG
α-SMA	GGGCATCCACGAAACCACCT	GAGCCGCCGATCCAGACAGA
TGF-β1	AACAATTCCTGGCGTTACCT	GCCCTGTATTCCGTCTCCTT
TGFβ1RI	GACCTTTGCCGATGCTTTCT	GACCTTTGCCGATGCTTTCT
TGFβ1RII	TGTGAGAAGCCGCAGGAAGT	CAGAGTGAAGCCGTGGTAGGT
Smad2	TTTGCCGAGTGCCTAAGTGA	AGGTTACAGCCTGGTGGGAT
Smad3	AGGGCTTTGAGGCTGTCTACC	CCCATTCAGGTGTAGCTCGAT
Smad7	ACTGGTGCGTGGTGGCATACT	CCGATCTTGCTCCTCACTTTCTG
β-actin	CACTGTGCCCATCTACGAGG	TAATGTCACGCACGATTTCC

α-SMA, α-Smooth muscle actin; β-actin, β-non-muscle; TGF-β1, transforming growth factor-β1; TGFβR, transforming growth factor-βreceptor.

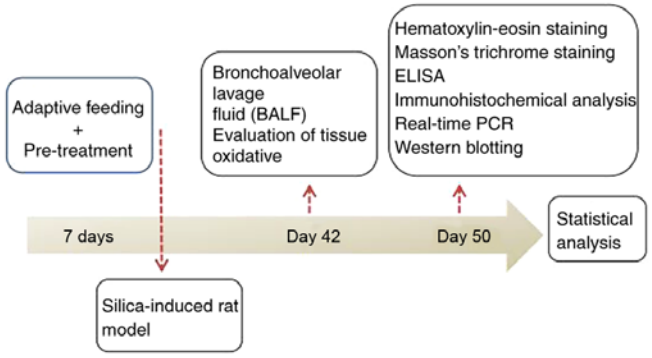

Figure 1. Flowchart of animal experimental procedures. BALF, bronchoalveolar lavage fluid.

followed by 30 cycles of 95˚C for 30 sec, 56˚C for 30 sec and extension step at 72˚C for 1 min. The sequences of the primers are presented in Table I.

Western blotting. According to the manufacturer's protocol (20), proteins were extracted using RIPA Lysis Buffer (Beyotime Institute of Biotechnology) and concentration was measured using a bicinchoninic acid assay. Protein samples (30 μg) were loaded on an 8% SDS-gel, resolved using SDS-PAGE and transferred to a PVDF membrane. After blocking with 5% non-fat dry milk for 2.5 h at 37˚C, the PVDF membrane was incubated with primary antibodies: TGF-β1 (1:500; cat. no. WL01076a; Wanleibio), TGFβ1RI (1:400; cat. no. WL03150; Wanleibio), TGFβ1RII (1:500; cat. no. A1415; ABclonal), Smad2 (1:500; cat. no. WL02286; Wanleibio), phospho-(p-)Smad2 (1:1,000; cat. no. E-AB-21129; Elabscience), Smad3 (1:500; cat. no. ab52903; Abcam), p-Smad3 (1:1,000; cat. no. ab52903; Abcam) or Smad7 (1:1,000; cat. no. WL02975; Wanleibio) overnight at 4˚C. The following day, the protein samples were incubated with an IgG antibody (1:500; cat. no. ab254262,; Abcam) at room temperature for 45 min. Signals were visualized using ECL reagent, and densitometry analysis was performed using Gel-Pro-Analyzer version 4.0 (Media Cybernetics, Inc.).

Statistical analysis. SPSS version 19.0 (IBM Corp.) was used to analyze all the data. Data are presented as the mean ± standard deviation. Differences amongst multiple groups were statistically analyzed using a one-way ANOVA with a post hoc Bonferroni test. $P<0.05$ was considered to indicate a statistically significant difference.

Results

ASV alleviates silica-induced pulmonary fibrosis in silicosis rats. H&E staining was performed to examine the pathological changes in the lung. As shown in Fig. 2A, compared with the control group, severe inflammatory damage was observed in the silicosis group, including infiltration of inflammatory cells, fused alveolar walls, as well as injury and thickening of the bronchial epithelial cell lining. However, when treated with ASV, these symptoms were significantly alleviated. Masson's trichrome staining was used to observe the changes in collagen fibers and ECM secretion in lung tissue (Fig. 2B). In the disease model group, notable fibrosis and strong collagen deposition were observed, and these pathological changes were alleviated in the ASV treated group.

ASV treatment reduces the expression of Collagen I, fibronectin and α-SMA. To evaluate the role of ASV on silica-induced fibroblast fibrosis, the changes in the expression of Collagen I, fibronectin and α-SMA were determined. As shown in Fig. 3A, increased mRNA expression levels of Collagen I, fibronectin and α-SMA were observed in the silicosis group compared with the control group (all $P<0.05$). Notably, ASV treatment significantly reduced the mRNA expression levels of these genes ($P<0.05$). Furthermore, immunohistochemistry was performed to verify these results, and the results showed that the staining was notably stronger in the silicosis group and weaker in the silicosis + ASV group (Fig. 3B). Accordingly, the mean density of Collagen I, fibronectin and α-SMA in the lung tissue increased significantly in the silicosis group when compared with that in the control group ($P<0.05$; Fig. 3C).

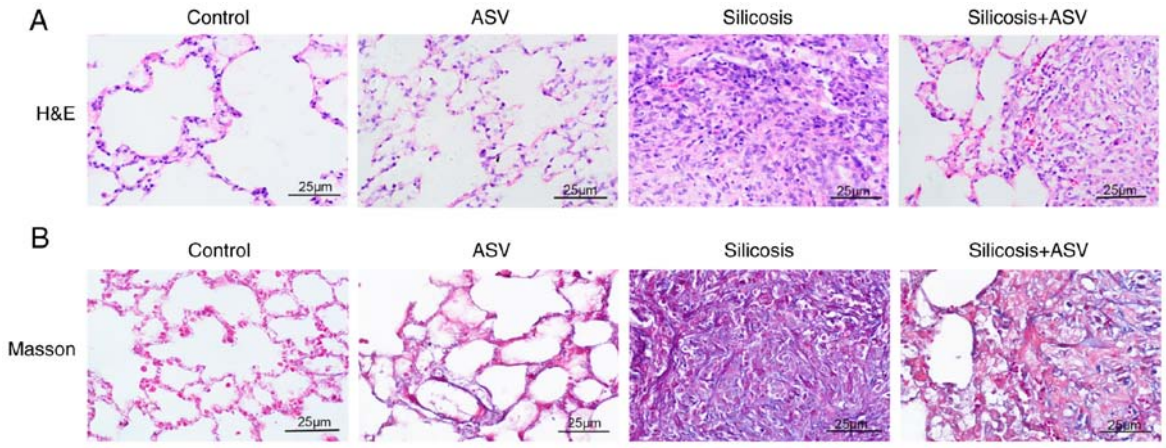

Figure 2. ASV alleviates silica-induced pulmonary fibrosis in silicosis rats. (A) H&E staining of lung sections in different groups. (B) Masson's trichrome staining of lung sections in different groups. Magnification, x400. Scale bar, 25 μm. ASV, astragaloside IV; H&E, hematoxylin and eosin.

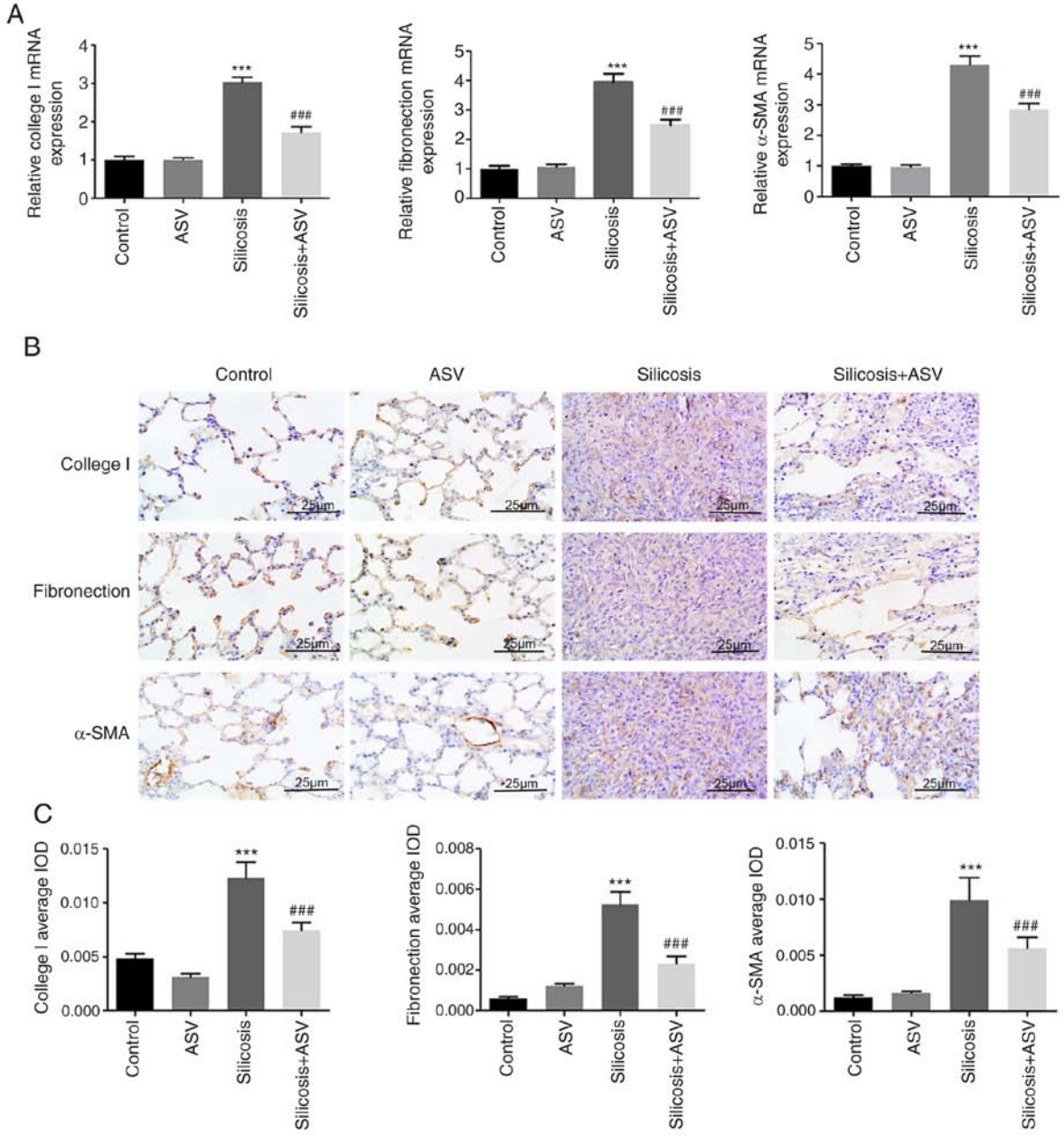

Figure 3. ASV treatment reduces the expressions of Collagen I, fibronectin and α-SMA. (A) mRNA expression of Collagen I, fibronectin and α-SMA. (B) Immunohistochemical staining of lung sections in different groups. Magnification, x400. Scale bar, 25 μm. (C) Average IOD of Collagen I, fibronectin and α-SMA in different groups. ***P<0.001 vs. Control; $^{###}$P<0.001 vs. Silicosis. α-SMA, α-smooth muscle actin; ASV, astragaloside IV; IOD, integral light density.

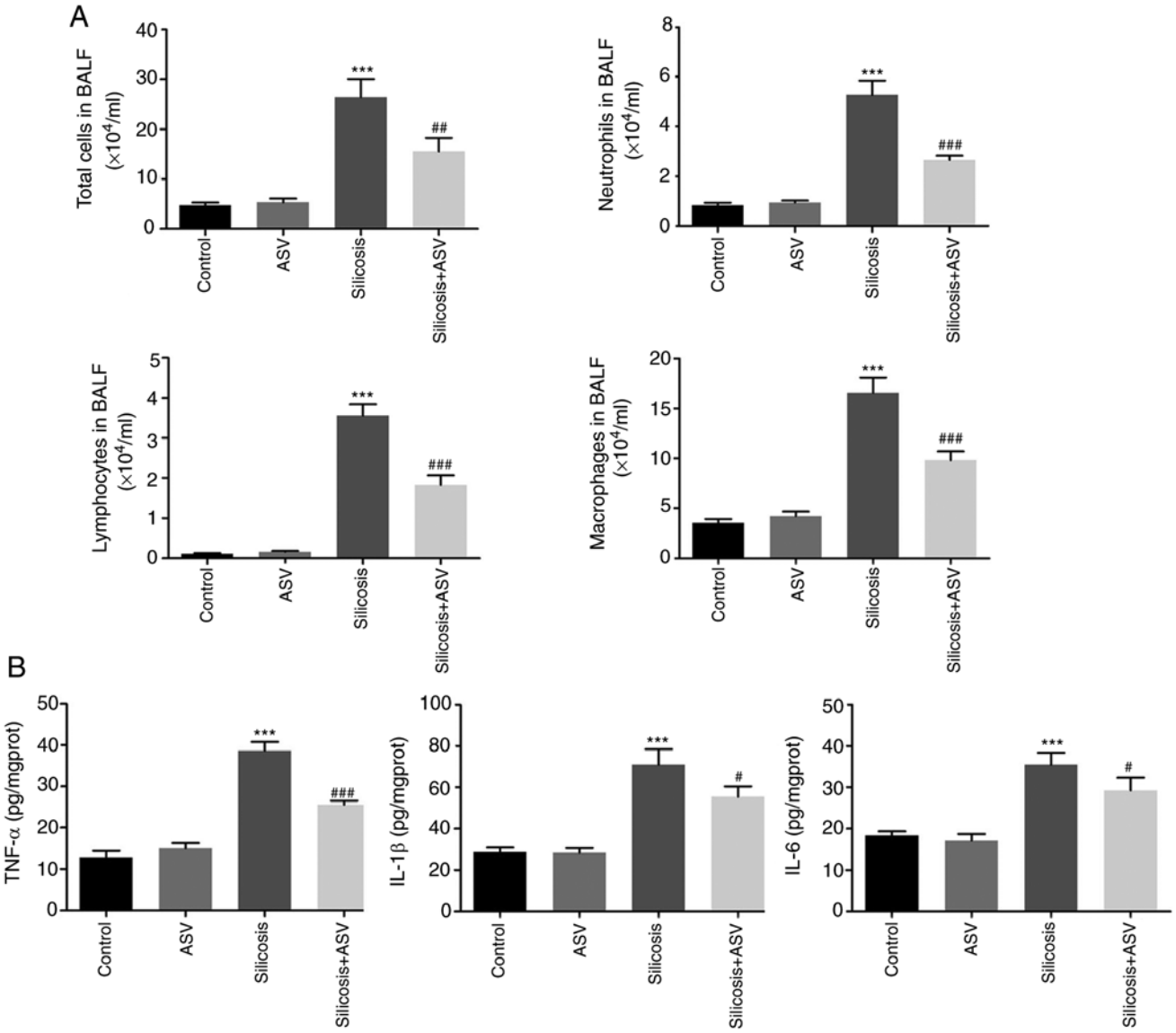

Figure 4. ASV-mediates an anti-pulmonary fibrosis response via a reduction in inflammation. (A) Cytological BALF parameters, including total cell, neutrophil, lymphocyte and macrophage counts, were significantly increased in the Silicosis group compared with the control group. ASV treatment significantly decreased the levels of these parameters. (B) ASV decreased the levels of inflammatory cytokines: TNF-α, IL-1β and IL-6. ***P<0.001 vs. Control; $^{\#}$P<0.05, $^{\#\#}$P<0.01, $^{\#\#\#}$P<0.001 vs. Silicosis. ASV, astragaloside IV; BALF, bronchoalveolar lavage fluid; TNF-α, tumor necrosis factor-α; IL, interleukin.

ASV-mediates an anti-pulmonary fibrosis response via reduction in inflammation. As shown in Fig. 4A, the cytological characteristics of BALF were affected by the administration of silica. Specifically, the total cell, neutrophil, lymphocyte and macrophage counts in the silicosis group were notably increased compared with the control group (all P<0.05). By contrast, the addition of ASV significantly decreased the total cell, neutrophil, lymphocyte and macrophage counts when compared with the silicosis group (all P<0.05).

Furthermore, the levels of TNF-α, IL-1β and IL-6 in lung tissues were quantified using ELISA. As shown in Fig. 4B, compared with the control group, silica exposure significantly increased the levels of TNF-α, IL-1β and IL-6 in lung tissues (all P<0.05). However, treatment with ASV resulted in a significant downregulation in the levels of these cytokines (all P<0.05).

ASV-mediates an anti-pulmonary fibrosis response via reduction of oxidative stress. As shown in Fig. 5A and B, the ROS levels and MDA concentration in the silicosis group were significantly higher compared with the control group, and treatment with ASV significantly decreased the ROS and MDA levels when compared with the silicosis group (all P<0.05). Furthermore, there was a significant decrease in the SOD and GSH-px concentrations in the silicosis group compared with the control group (P<0.05). However, following treatment with ASV, an increase in SOD and GSH-px levels was observed (Fig. 5C and D).

ASV suppresses silica-induced lung fibrosis via the TGF-β1-Smads signaling pathway. The TGF-β/Smads signaling pathway is well-established as the primary pathway underlying pulmonary fibrosis (21). To further explore whether ASV exerted its anti-fibrotic effect via this signaling pathway, the mRNA and protein expression levels of genes associated with this pathway were assessed. At the transcriptional level, the expression of TGF-β1, TGFβ1RI and TGFβ1RII increased significantly following exposure to silica (Fig. 6A). Amongst

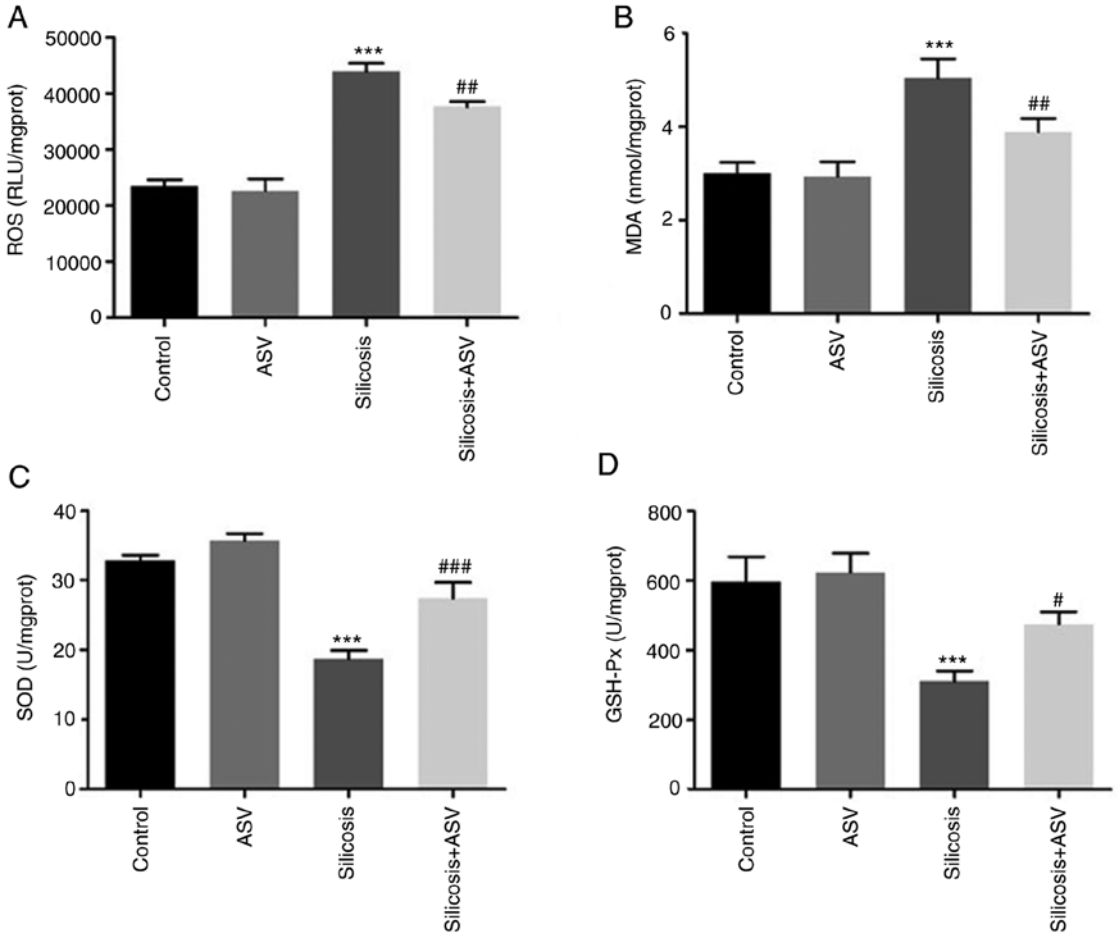

Figure 5. ASV-mediates an anti-pulmonary fibrosis response via reduction of oxidative stress. (A) ROS, (B) MDA, (C) SOD and (D) GSH-px levels in the different groups. ***P<0.001 vs. Control; $^{\#}$P<0.05, $^{\#\#}$P<0.01, $^{\#\#\#}$P<0.001 vs. Silicosis. MDA, malondialdehyde; ROS, oxygen species; SOD, superoxide dismutase; GSH-px, glutathione peroxidase; ASV, astragaloside IV.

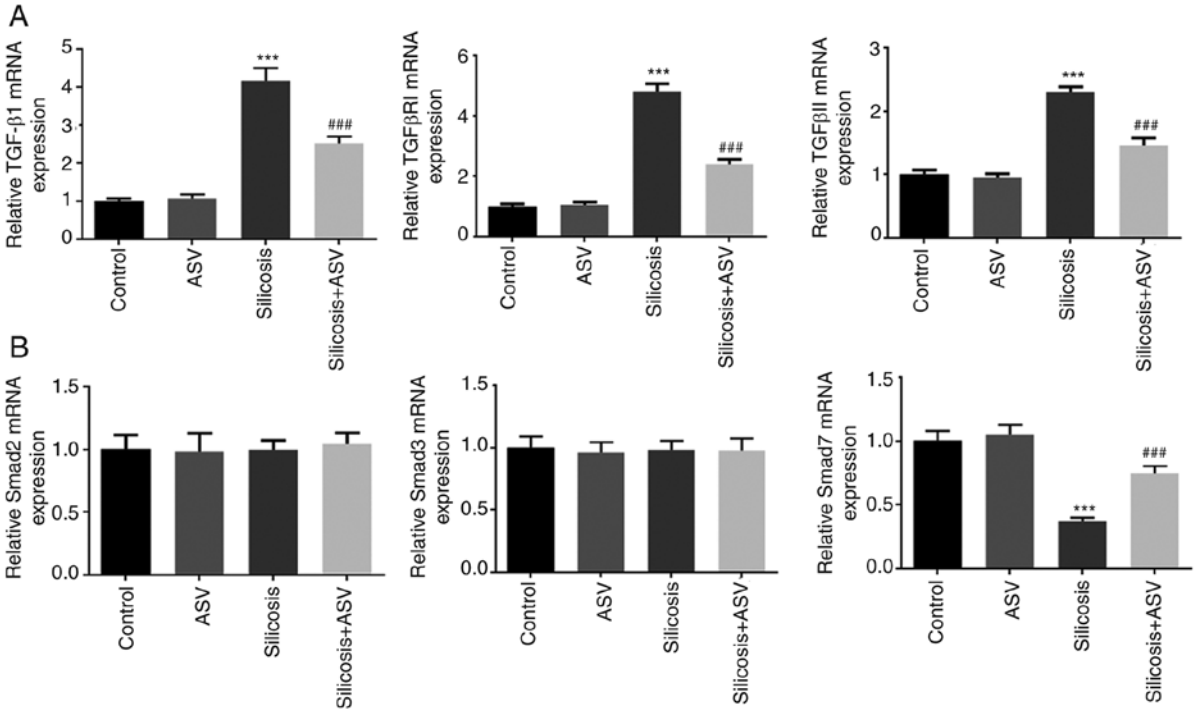

Figure 6. ASV suppresses silica-induced pulmonary fibrosis via the TGF-β1-Smads signaling pathway. mRNA expression levels of (A) TGF-β1, TGFβRI and TGFβRII; and (B) Smad2, Smad3 and Smad7. ***P<0.001 vs. Control; $^{\#\#\#}$P<0.001 vs. Silicosis. ASV, astragaloside IV; TGF-β1, transforming growth factor-β1; TGFβR, transforming growth factor-β receptor.

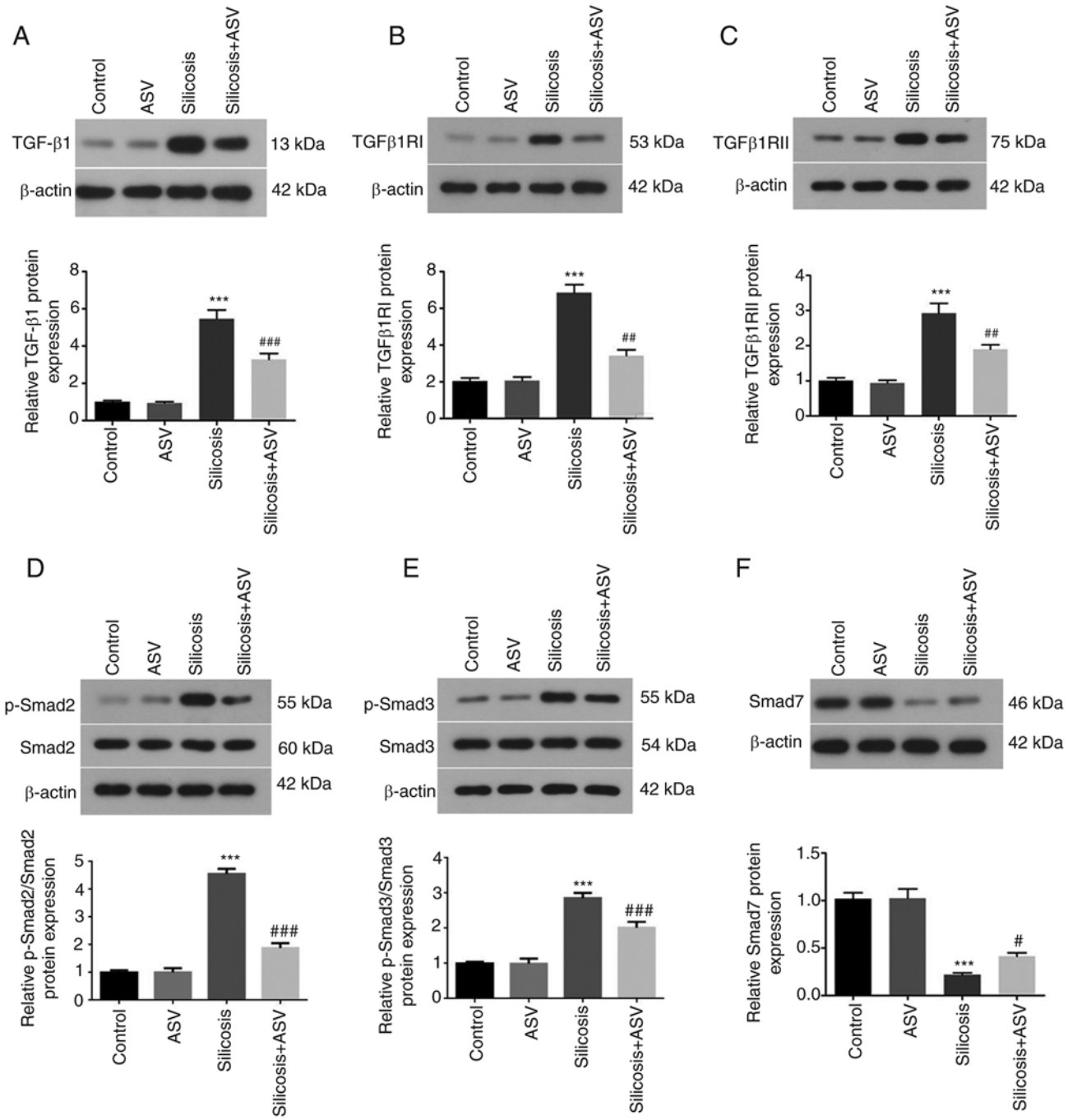

Figure 7. ASV suppresses silica-induced pulmonary fibrosis via the TGF-β1-Smads signaling pathway. Protein expression of (A) TGF-β1, (B) TGFβRI, (C) TGFβRII; (D) p-Smad2/Smad2; (E) p-Smad3/Smad3, and (F) Smad7. ***P<0.001 vs. Control; $^{\#}$P<0.05, $^{\#\#}$P<0.01, $^{\#\#\#}$P<0.001 vs. Silicosis. ASV, astragaloside IV; TGF-β1, transforming growth factor-β1; TGFβR, transforming growth factor-β receptor; p-, phospho.

the downstream genes, there were no statistically significant differences in Smad2 and Smad3 in any of the groups; however, the mRNA expression levels of Smad7 were significantly downregulated (P<0.05). Interestingly, the administration of ASV reversed the changes in the expression of the above genes (Fig. 6B).

As shown in Fig. 7A-E, the protein expression levels of TGF-β1, TGFβ1RI, TGFβ1RII, p-Smad2/Smad2 and p-Smad3/Smad3 were significantly increased in the Silicosis group compared with the Control group, whereas the Smad7 protein expression levels were decreased significantly (P<0.05). Treatment with ASV significantly decreased the protein expression levels of TGF-β1, TGFβ1RI, TGFβ1RII, p-Smad2/Smad2 and p-Smad3/Smad3, and increased the expression of Smad7 protein when compared the Silicosis group.

Discussion

A large body of data suggests that activated fibroblasts serve a critical role in driving the development of pulmonary fibrosis (22,23). Fibroblasts express high levels of α-SMA, fibronectin and collagen, andpromote wound healing and fibrosis remodeling. In addition, fibroblasts can cause excessive

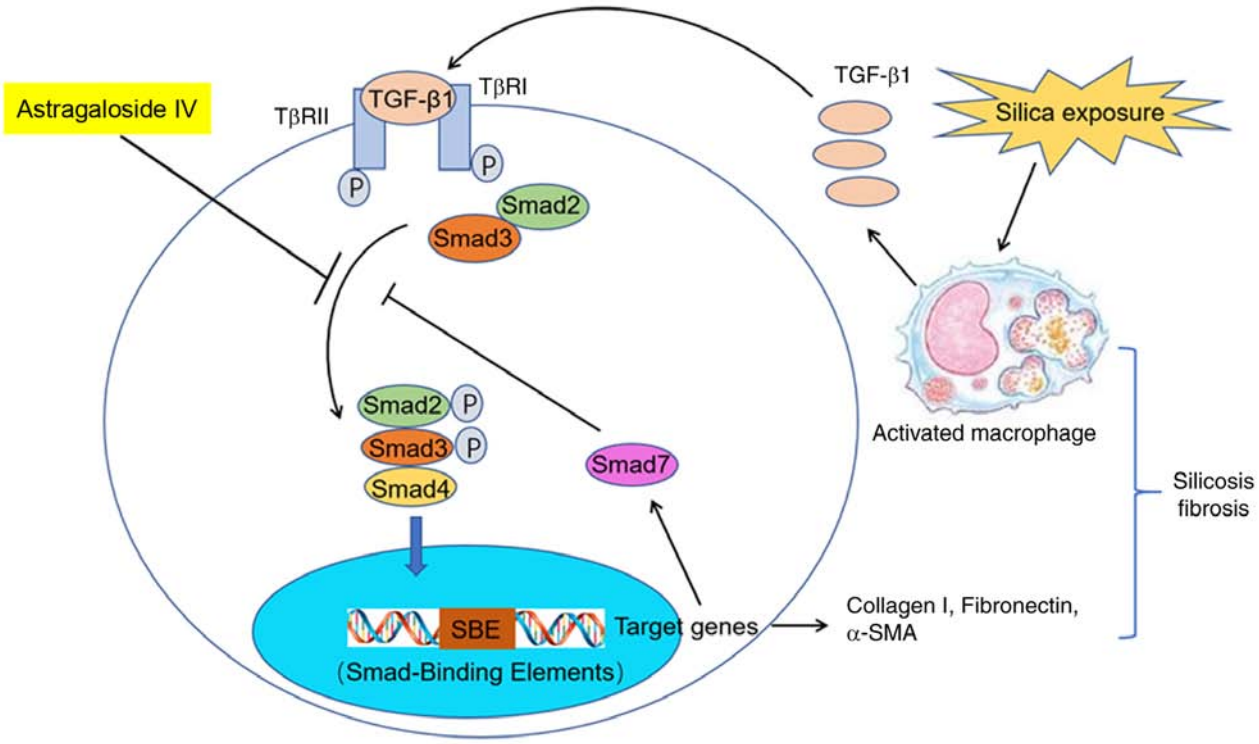

Figure 8. Schematic diagram showing how ASV alleviates silica-induced pulmonary fibrosis by regulating TGF-β1/Smads pathway. ASV, astragaloside IV; TGF-β1, transforming growth factor-β1; TGFβR, transforming growth factor-β receptor; α-SMA, α-smooth muscle actin.

deposition of ECM (collagen I and collagen III) (24). In the present study, it was shown that exposure to silica caused severe pathological damage to lung tissues, including increased formation of lung nodules, increased infiltration of inflammatory cells, and thickening of the alveolar walls and bronchial epithelial cells. However, treatment with ASV alleviated these symptoms. Furthermore, it was shown that ASV treatment reduced the expression of Collagen I, fibronectin and α-SMA, consistent with a previous study, in which it was shown that a-SMA, Collagen I, Collagen III, FSP-1, fibronectin and Vimentin ablation attenuated fibrosis in lung tissue samples from mice (25). Collectively, the above data showed that ASV delayed silica-induced pulmonary fibrosis and that it possesses anti-silicosis fibrosis effects.

Accumulating evidence has indicated that silica induces inflammatory responses, including the secretion of inflammatory factors (26) and infiltration of inflammatory cells (27). In the present study, it was shown that in the silicosis group, total cell counts, as well as the neutrophil, lymphocyte and macrophage counts were high. Interestingly, ASV treatment reduced the expression of these cytological markers of lung injury. Additionally, the potential role of androgens in targeting neutrophils, lymphocytes and macrophages was determined, which is evident in the reduction of inflammatory cell infiltration. A study by Hou *et al* (28) showed that exposure to crystalline silica particles increased TNF-α, IL-1β and IL-6, levels, amongst other cytokines. TNF-α can accelerate EMT and up-regulates TGF-β1 expression in primary mouse lung fibroblasts (29) IL-1β can stimulate collagen expression and notably induces tissue destruction, accompanied by increased inflammation and collagen deposition (30). Consistent with the *in vivo* experiments, silicosis rats given ASV exhibited decreased levels of TNF-α, IL-1β and IL-6 in BALF, suggesting that ASV can delay the progression of pulmonary fibrosis by reducing the inflammatory response in lung tissues.

Oxidative stress is one of the key features of silica induced pulmonary fibrosis. Related studies have shown that the contact between alveolar macrophages and silica during the inflammatory process can produce oxidase, leading to the production of high levels of ROS, thereby further promoting inflammation in a feed-forward loop (31,32). Continued ROS production can cause phagocytic cell death, inflammatory cell recruitment and silica deposition, and cause irreversible lung damage (33). MDA is an indicator of oxidative stress. It reflects the quantities of oxidized free radicals in the body to a certain extent, and indirectly reflects the degree of oxidative stress, which is negatively correlated with lung function (34), and may lead to irreversible lung injury (27). Antioxidants, such as GSH-px and SOD, can not only resist the direct damage caused by oxidants, but also alters the course of inflammatory events associated with chronic lung diseases (27). In the present study, following exposure to silica, there was a significant decrease in GSH-px and SOD levels, as well as a significant increase in the levels of ROS and MDA in silicotic patients. Conversely, ASV reversed the expression of the above factors, suggesting that ASV could inhibit pulmonary fibrosis by reducing oxidative stress.

There is evidence that TGF-β1 can regulate epithelial cell apoptosis, fibroblast proliferation, myofibroblast differentiation and collagen synthesis, thus it may be essential in the progression of lung fibrosis in mice (35). In addition, TGF-β1 is upregulated in lung tissues of patients with pulmonary fibrosis and overexpression of active TGF-β1 induces prolonged and severe interstitial lung fibrosis in rats (36). TGF-β1 is known

to serve its pro-fibrotic role by activating downstream mediators, including Smad2 and Smad3, and is negatively regulated by Smad7 expression (7,8). Specifically, TGF-β1 initially binds to TGF-βII phosphorylating it to activate TGFβRI. Subsequently, Smad2 and Smad3 are phosphorylated and activated by TGFβRI. The phosphorylated Smad2 and Smad3 binds to Smad4 to form the Smads complex, which is transferred to the nucleus by cytoplasmic nuclear transporters and acts on the TGF-β1 target gene to regulate transcription of target genes. When the external stimulus inducing the signal ends, p-Smads are rapidly dephosphorylated, and the Smads protein in the cytoplasm and nucleus is rapidly metabolized by the ubiquitin-proteasome system, returning the cytoplasmic levels to resting levels (29). Under pathological conditions, the p-Smad2/Smad2 ratio and p-Smad3/Smad3 ratio are increased. Chang *et al* (37) showed that following exposure to 100 μg/ml nano NiO, the phosphorylation levels of Smad2 and Smad3 genes and proteins in A549 cells both increased, suggesting that NiO leads to abnormal changes in Smad2 and Smad3. Consistent with previous studies, silica increased the expression of TGF-β1, TGF-βRI, TGF-βII, p-Smad2/Smad2 and p-Smad3/Smad3, and decreased Smad7 levels in the present study. Interestingly, the addition of ASV reversed the expression of these genes to a certain extent. Collectively, the data indicated that ASV can inhibit silica-induced pulmonary fibrosis by promoting negative feedback of the TGF-β1/Smads signaling pathway and inhibiting its positive feedback (Fig. 8).

In conclusion, ASV elicits its anti-pulmonary fibrotic effect by decreasing silica-induced pulmonary fibrosis inflammation and oxidative stress, and the mechanism underlying the effects of ASV may involve the TGF-β1/Smads pathway. Thus, ASV may serve as a promising treatment for the management of silicosis.

Acknowledgements

Not applicable.

Funding

This study was supported by the general project of National Natural Science foundation of China (grant no. 81973630) and a grant from the Tai'an City Technology Development Program (grant nos. 2019NS195 and 2018NS0170).

Availability of data and materials

The datasets used and/or analyzed during the present study are available from the corresponding author on reasonable request.

Authors' contributions

WW, NNL and KW conceived and designed the present study. FFF obtained the study materials and collected the patient data. NNL and LW performed the experiments. NNL and XZ analyzed and interpreted the data. All authors participated in writing the manuscript. All authors have read and approved the final manuscript. NNL and WW confirmed the authenticity of all the raw data. All authors read and approved the final manuscript.

Ethics approval and consent to participate

The present study was approved by the Ethics Committee of The Second Hospital of Shandong University. All procedures adhered to the recommendations described in the Guide for the Care and Use of Laboratory Animals of the National Institutes of Health.

Patient consent for publication

Not applicable.

Competing interests

The authors declare that they have no competing interests.

References

1. Zhao JQ, Li JG and Zhao CX: Prevalence of pneumoconiosis among young adults aged 24-44 years in a heavily industrialized province of China. J Occup Health 61: 73-81, 2019.
2. Ferrante P: Asbestosis and silicosis hospitalizations in Italy (2001-2015): Results from the national hospital discharge registry. Eur J Public Health 29: 876-882, 2019.
3. Reilly MJ, Timmer SJ and Rosenman KD: The burden of silicosis in michigan: 1988-2016. Ann Am Thorac Soc 15: 1404-1410, 2018.
4. Xu Q, Liu Y, Pan H, Xu T, Li Y, Yuan J, Li P, Yao W, Yan W and Ni C: Aberrant expression of miR-125a-3p promotes fibroblast activation via Fyn/STAT3 pathway during silica-induced pulmonary fibrosis. Toxicology 414: 57-67, 2019.
5. Hou X, Summer R, Chen Z, Tian Y, Ma J, Cui J, Hao X, Guo L, Xu H, Wang H and Liu H: Lipid uptake by alveolar macrophages drives fibrotic responses to silica dust. Sci Rep 9: 399, 2019.
6. Zhou Y, He Z, Gao Y, Zheng R, Zhang X, Zhao L and Tan M: Induced pluripotent stem cells inhibit bleomycin-induced pulmonary fibrosis in mice through suppressing TGF-β1/Smad-mediated epithelial to mesenchymal transition. Front Pharmacol 7: 430, 2016.
7. Li PF, He RH, Shi SB, Li R, Wang QT, Rao GT and Yang B: Modulation of miR-10a-mediated TGF-β1/Smads signaling affects atrial fibrillation-induced cardiac fibrosis and cardiac fibroblast proliferation. Biosci Rep 39: BSR20181931, 2019.
8. Lu Y, Zhang T, Shan S, Wang S, Bian W, Ren T and Yang D: MiR-124 regulates transforming growth factor-β1 induced differentiation of lung resident mesenchymal stem cells to myofibroblast by repressing Wnt/β-catenin signaling. Dev Biol 449: 115-121, 2019.
9. Bellaye PS, Shimbori C, Upagupta C, Sato S, Shi W, Gauldie J, Ask K and Kolb M: Lysyl oxidase-like 1 protein deficiency protects mice from adenoviral transforming growth factor-β1-induced pulmonary fibrosis. Am J Respir Cell Mol Biol 58: 461-470, 2018.
10. Li LC and Kan LD: Traditional Chinese medicine for pulmonary fibrosis therapy: Progress and future prospects. J Ethnopharmacol 198: 45-63, 2017.
11. Meng LQ, Tang JW, Wang Y, Zhao JR, Shang MY, Zhang M, Liu SY, Qu L, Cai SQ and Li XM: Astragaloside IV synergizes with ferulic acid to inhibit renal tubulointerstitial fibrosis in rats with obstructive nephropathy. Br J Pharmacol 162: 1805-1818, 2011.
12. Yu WN, Sun LF and Yang H: Inhibitory effects of astragaloside IV on bleomycin-induced pulmonary fibrosis in rats via attenuation of oxidative stress and inflammation. Inflammation 39: 1835-1841, 2016.
13. Wang L, Chi YF, Yuan ZT, Zhou WC, Yin PH, Zhang XM, Peng W and Cai H: Astragaloside IV inhibits renal tubulointerstitial fibrosis by blocking TGF-β/Smad signaling pathway in vivo and in vitro. Exp Biol Med (Maywood) 239: 1310-1324, 2014.
14. Sangomla S, Saifi MA, Khurana A and Godugu C: Nanoceria ameliorates doxorubicin induced cardiotoxicity: Possible mitigation via reduction of oxidative stress and inflammation. J Trace Elem Med Biol 47: 53-62, 2018.
15. Ohkawa H, Ohishi N and Yagi K: Assay for lipid peroxides in animal tissues by thiobarbituric acid reaction. Anal Biochem 95: 351-358, 1979.

16. Tsang CK, Liu Y, Thomas J, Zhang Y and Zheng XF: Superoxide dismutase 1 acts as a nuclear transcription factor to regulate oxidative stress resistance. Nat Commun 5: 3446, 2014.
17. Voicu SN, Balas M, Stan MS, Trică B, Serban AI, Stanca L, Hermenean A and Dinischiotu A: Amorphous silica nanoparticles obtained by laser ablation induce inflammatory response in human lung fibroblasts. Materials (Basel) 12: 1026, 2019.
18. Moron MS, Depierre JW and Mannervik B: Levels of glutathione, glutathione reductase and glutathione S-transferase activities in rat lung and liver. Biochim Biophys Acta 582: 67-78, 1979.
19. Wang J, Ni G, Liu Y, Han Y, Jia L and Wang Y: Tanshinone IIA promotes axonal regeneration in rats with focal cerebral ischemia through the inhibition of nogo-A/NgR1/RhoA/ROCKII/MLC signaling. Drug Des Devel Ther 14: 2775-2787, 2020.
20. Chen X, Chen Y, Hou Y, Song P, Zhou M, Nie M and Liu X: Modulation of proliferation and differentiation of gingiva-derived mesenchymal stem cells by concentrated growth factors: Potential implications in tissue engineering for dental regeneration and repair. Int J Mol Med 44: 37-46, 2019.
21. Li N, Feng F, Wu K, Zhang H, Zhang W and Wang W: Inhibitory effects of astragaloside IV on silica-induced pulmonary fibrosis via inactivating TGF-β1/Smad3 signaling. Biomed Pharmacother 119: 109387, 2019.
22. Bagnato G and Harari S: Cellular interactions in the pathogenesis of interstitial lung diseases. Eur Respir Rev 24: 102-114, 2015.
23. Li J, Yao W, Hou JY, Zhang L, Bao L, Chen HT, Wang D, Yue ZZ, Li YP, Zhang M and Hao CF: Crystalline silica promotes rat fibrocyte differentiation in vitro, and fibrocytes participate in silicosis in vivo. Biomed Environ Sci 30: 649-660, 2017.
24. Phillips RJ, Burdick MD, Hong K, Lutz MA, Murray LA, Xue YY, Belperio JA, Keane MP and Strieter RM: Circulating fibrocytes traffic to the lungs in response to CXCL12 and mediate fibrosis. J Clin Invest 114: 438-446, 2004.
25. Cheng F, Shen Y, Mohanasundaram P, Lindström M, Ivaska J, Ny T and Eriksson JE: Vimentin coordinates fibroblast proliferation and keratinocyte differentiation in wound healing via TGF-β-Slug signaling. Proc Natl Acad Sci USA 113: E4320-E4327, 2016.
26. Stan MS, Sima C, Cinteza LO and Dinischiotu A: Silicon-based quantum dots induce inflammation in human lung cells and disrupt extracellular matrix homeostasis. FEBS J 282: 2914-2929, 2015.
27. Huang H, Chen M, Liu F, Wu H, Wang J, Chen J, Liu M and Li X: N-acetylcysteine tiherapeutically protects against pulmonary fibrosis in a mouse model of silicosis. Biosci Rep 39: BSR20190681, 2019.
28. Hou J, Ma T, Cao H, Chen Y, Wang C, Chen X, Xiang Z and Han X: TNF-α-induced NF-κB activation promotes myofibroblast differentiation of LR-MSCs and exacerbates bleomycin-induced pulmonary fibrosis. J Cell Physiol 233: 2409-2419, 2018.
29. Zheng ZC, Zhu W, Lei L, Liu XQ and Wu YG: Wogonin ameliorates renal inflammation and fibrosis by inhibiting NF-κB and TGF-β1/Smad3 signaling pathways in diabetic nephropathy. Drug Des Devel Ther 14: 4135-4148, 2020.
30. Song C, He L, Zhang J, Ma H, Yuan X, Hu G, Tao L, Zhang J and Meng J: Fluorofenidone attenuates pulmonary inflammation and fibrosis via inhibiting the activation of NALP3 inflammasome and IL-1β/IL-1R1/MyD88/NF-κB pathway. J Cell Mol Med 20: 2064-2077, 2016.
31. Robinson JM: Reactive oxygen species in phagocytic leukocytes. Histochem Cell Biol 130: 281-297, 2008.
32. Mittal M, Siddiqui MR, Tran K, Reddy SP and Malik AB: Reactive oxygen species in inflammation and tissue injury. Antioxid Redox Signal 20: 1126-1167, 2014.
33. Lopes-Pacheco M, Ventura TG, de Oliveira HD, Monção-Ribeiro LC, Gutfilen B, de Souza SAL, Rocco PRM, Borojevic R, Morales MM and Takiya CM: Infusion of bone marrow mononuclear cells reduces lung fibrosis but not inflammation in the late stages of murine silicosis. PLoS One 9: e109982, 2014.
34. Kluchová Z, Petrásová D, Joppa P, Dorková Z and Tkácová R: The association between oxidative stress and obstructive lung impairment in patients with COPD. Physiol Res 56: 51-56, 2007.
35. Liu H, Fang S, Wang W, Cheng Y, Zhang Y, Liao H, Yao H and Chao J: Macrophage-derived MCPIP1 mediates silica-induced pulmonary fibrosis via autophagy. Part Fibre Toxicol 13: 55, 2016.
36. Guo J, Fang Y, Jiang F, Li L, Zhou H, Xu X and Ning W: Neohesperidin inhibits TGF-β1/Smad3 signaling and alleviates bleomycin-induced pulmonary fibrosis in mice. Eur J Pharmacol 864: 172712, 2019.
37. Chang X, Tian M, Zhang Q, Gao J, Li S and Sun Y: Nano nickel oxide promotes epithelial-mesenchymal transition through transforming growth factor β1/smads signaling pathway in A549 cells. Environ Toxicol 35: 1308-1317, 2020.